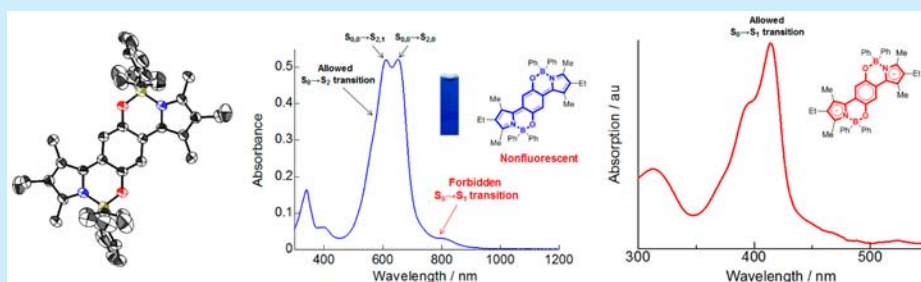


Synthesis, Absorption, and Electrochemical Properties of Quinoid-Type Bisboron Complexes with Highly Symmetrical Structures

Yasuhiro Kubota,^{*,†} Takahiro Niwa,[†] Jiye Jin,[‡] Kazumasa Funabiki,[†] and Masaki Matsui^{*,†}[†]Department of Chemistry and Biomolecular Science, Faculty of Engineering, Gifu University, Yanagido, Gifu 501-1193, Japan[‡]Department of Chemistry, Faculty of Science, Shinshu University, 3-1-1 Asahi, Matsumoto, Nagano 390-8621, Japan

S Supporting Information



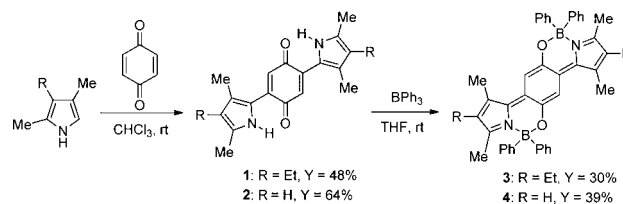
ABSTRACT: Novel bisboron complexes of bidentate ligands consisting of 1,4-benzoquinone and two pyrrole rings were synthesized by using a simple two-step reaction. In solution, the bisboron complexes showed absorption maxima at ~620 and 800 nm, which were attributed to the allowed $S_0 \rightarrow S_2$ and forbidden $S_0 \rightarrow S_1$ transitions, respectively. The bisboron complexes did not show any fluorescence, probably because of their highly symmetrical structure which forbids the $S_0 \rightarrow S_1$ transition. Bisboron complexes underwent a two-electron reduction to yield the corresponding aromatic dianion, which showed absorption maxima at ~410 nm.

Near-infrared (NIR) absorbing dyes are important as heat absorbers, optical filters, charge-generation materials, information-storage materials, and photosensitizers for photodynamic therapy and solar cells.¹ Rylene diimides,^{2a} polymethines,^{2b} phthalocyanines,^{2c} quinones,^{1a} azo dyes,^{1a} triaryl-methane dyes,^{2d} and donor–acceptor dyes^{1b} are known as NIR absorbing dyes.

On the other hand, organoboron compounds are attracting increased attention because of their potential applications for fluorescent materials.³ Recently, Wang et al.,⁴ Ziessel et al.,⁵ and other groups⁶ have reported that the boron complexes of the $N^{\wedge}O$ ligand based on phenol ring exhibit fluorescence and can be applied as organic light-emitting diodes and fluorescent labeling reagents. During our studies on the development of fluorescent boron complexes,⁷ we became interested in the synthesis of the boron complexes of 1,4-benzoquinone-based ligands, which are oxidized analogues of the previously reported fluorescent boron complexes based on benzene-1,4-diol by Zhang et al. as potential candidates for NIR absorbing and fluorescent dyes (Figure S1, Supporting Information).^{4a,b} In this paper, we report the synthesis, absorption, and electrochemical properties of novel quinoid-type boron complexes with highly symmetrical structures.

The synthesis of the target complex, quinoid-type bisboron **3**, was carried out by a simple two-step reaction (Scheme 1). Bis(pyrrol-2-yl)-1,4-benzoquinone **1** was synthesized according to the previously reported method.⁸ The reaction of **1** with 2 equiv of triphenylborane in THF afforded bisboron complex **3** in

Scheme 1. Synthesis of Quinoid-Type Bisboron Complexes



a 30% yield. A plausible mechanism for this reaction is shown in Scheme S1. When the reaction was carried out using 1 equiv of triphenylborane, bisboron complex **3** was obtained in a 20% yield, and 29% of starting material **1** was recovered. However, monoboron complex **5** was not obtained. This indicates that **5** is more reactive than **1** toward triphenylborane and/or **5** is unstable toward isolation. Bisboron complex **4** was also obtained by a similar reaction (Scheme 1).

The crystal structures of **3** and **4** were confirmed by single-crystal X-ray analyses (Figure 1 and Figure S2). The chromophore consisting of the central quinone moiety and two pyrrole rings is almost planar. The B1 and B1* atoms are located slightly above and below the plane. The two phenyl rings on B1 and B1* atoms are oriented perpendicularly above and

Received: May 27, 2015

Published: June 11, 2015

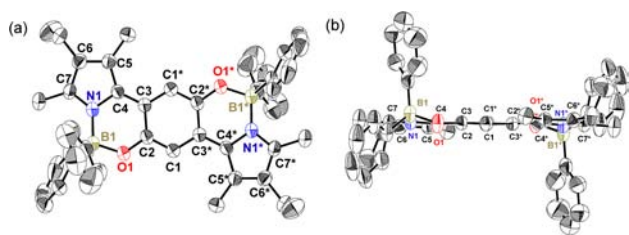


Figure 1. ORTEP view of **3**. (a) Top view and (b) side view. Hydrogen atoms are omitted for clarity.

below the plane; the other two phenyl rings are oriented almost horizontally in the plane.

The bond lengths of **1**^{8b} and **3** are shown in Figure S3. Both **1** and **3** show high symmetry (S_2 symmetry). The C2*–O1* (1.333 Å) and C1*–C3 (1.427 Å) bond lengths of the quinone moieties of **3** are considerably longer than those of **1** (C2*–O1*: 1.242 Å and C1*–C3: 1.340 Å). The C1*–C2* bond length of **3** (1.370 Å) is shorter than that of **1** (1.433 Å). Therefore, the quinone moiety of **3** is considered to have an enolate structure rather than an enone structure. The bond linking the quinone moiety and pyrrole ring of **3** (C3*–C4*: 1.396 Å) is shorter than that of **1** (1.434 Å). Furthermore, the difference in the bond lengths in the pyrrole rings between **1** and **3** indicates that the pyrrole rings of **3** possess a 2*H*-pyrrole structure in preference to a 1*H*-pyrrole structure. These results indicate that bisboron complex **3** has a highly conjugated quinoid structure.

The UV–vis absorption spectra of **1–4** in toluene are shown in Figure 2. Bisboron complex **3** (612 and 644 nm) shows a

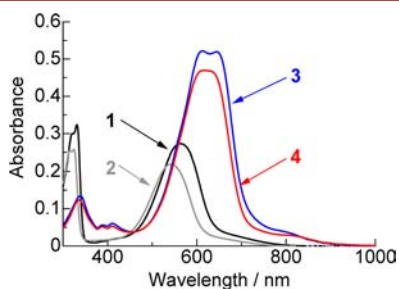


Figure 2. UV–vis absorption spectra of **1–4** in toluene.

significantly red-shifted absorption maximum (λ_{\max}) compared to ligand **1** (563 nm). The molar extinction coefficients (ϵ) of **3** (52200 at 612 nm and 52000 at 644 nm) are higher than that of **1** (27300 at 563 nm). The bathochromic shifts and higher ϵ values of **3** are because of its highly conjugated structure.

The effect of solvent on the absorption properties of **3** was studied (Figure S4 and Table S1). Two absorption peaks were observed at \sim 620 nm only in nonpolar solvents such as *n*-hexane and toluene. In more polar solvents, **3** showed one absorption peak at \sim 600 nm. Therefore, the observed λ_{\max} at 612 nm in toluene can be attributed to the vibrational band of the absorption at 644 nm. The observed vibrational transition is because of the exclusion of solvent relaxation in nonpolar solvents.⁹ Bisboron complex **3** showed a slightly negative solvatochromism, indicating that the dipole moment of the Frank–Condon excited state is slightly lower than that of the equilibrium ground state. Similar trends were observed for **4** (Figures S5 and Table S1).

In order to better understand the absorption properties, the density functional theory (DFT) calculations were performed

with the Gaussian 09 software package.¹⁰ The geometry optimizations and time-dependent DFT (TDDFT) calculations of **3** were performed using the B3LYP/6-31G(d,p) method. The calculated molecular orbitals of **3** are shown in Figure 3. The calculated λ_{\max} , main orbital transition, and oscillator strength f are listed in Table 1.

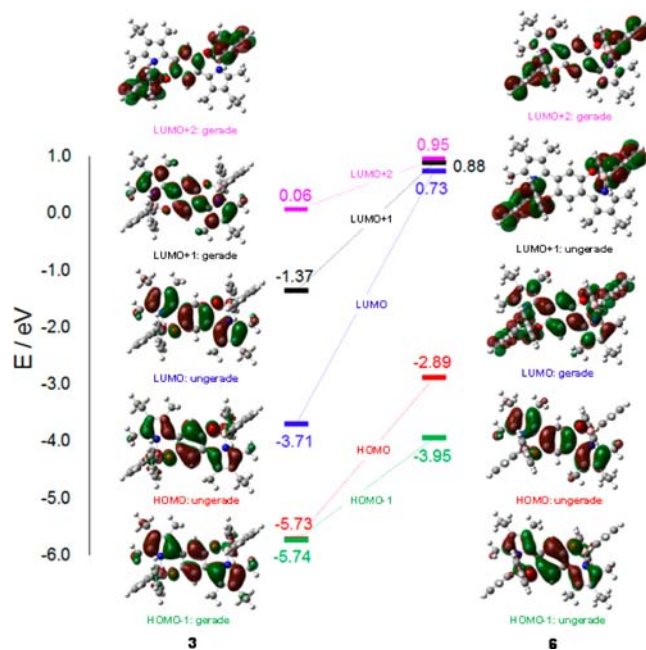


Figure 3. Molecular orbital energy diagram and isodensity surface plots of **3** and its dianion **6**.

Table 1. TDDFT Calculations at the B3LYP/6-31G(d,p) Level and Experimentally Obtained Absorption Properties

compd	transition	λ_{\max}^c (nm)	main orbital transition	f	λ_{\max}^d (ϵ) (nm)
3 ^a	$S_0 \rightarrow S_1$	788	HOMO to LUMO (0.71)	0.00	790 (4000)
	$S_0 \rightarrow S_2$	625	HOMO–1 to LUMO (0.60)	0.71	612 (52200) 644 (52000)
6 ^b	$S_0 \rightarrow S_1$	393	HOMO to LUMO (0.70)	0.45	414
	$S_0 \rightarrow S_2$	379	HOMO to LUMO + 1 (0.70)	0.00	<i>e</i>
	$S_0 \rightarrow S_3$	370	HOMO to LUMO + 2 (0.70)	0.35	395

^aToluene was used as solvent in the calculation. ^bTHF was used as solvent in the calculation. ^cCalculated absorption maximum. ^dObserved absorption maximum. ^eNot observed.

The $S_0 \rightarrow S_1$ transition of **3** is mostly attributed to the HOMO–LUMO transitions; the λ_{\max} value of **3** is estimated to be 788 nm. However, despite the fact that the HOMO and LOMO have spatial overlap, the transition was not allowed ($f = 0.00$). According to the Laporte's parity selection rule, gerade–gerade and ungerade–ungerade optical transitions are forbidden.¹¹ The HOMO and LUMO of **3** are ungerade (Figure 3). Therefore, the forbidden transition between the HOMO and LUMO can be attributed to the parity forbidden caused by their highly symmetrical structure. In the UV–vis spectra of **3**, a broad peak was observed at \sim 800 nm (Figure 2). The broad absorption

may be due to the forbidden $S_0 \rightarrow S_1$ transition. The experimentally observed λ_{max} value of **3** (612 and 644 nm) can be assigned to the $S_0 \rightarrow S_2$ transition, which mainly corresponds to the HOMO–1 to LUMO transition (Table 1). Because the λ_{max} of **3** at 612 nm is attributed to the vibrational band of the absorption at 644 nm, the peaks at 612 and 644 nm are attributed to the $S_{0,0} \rightarrow S_{2,1}$ and $S_{0,0} \rightarrow S_{2,0}$ transitions, respectively.

The absorption spectra of **3** and **4** were also measured in the solid state mixed with potassium bromide (Figure S6). Bisboron complexes **3** and **4** showed a pronounced absorption in the NIR region (up to 1600 nm). This indicates that quinoid-type bisboron complexes have potential application in NIR absorbing dyes such as dye-sensitized solar cells. To obtain the thermal properties, TG–DTA measurements of **3** and **4** were preformed (Figures S7 and S8). Bisboron complexes **3** and **4** were decomposed without showing a melting point. The decomposition temperatures were as follows: **3** (236 °C) and **4** (235 °C).

Unlike in the case of the previously reported benzene-1,4-diol analogues by Zhang et al.,^{4a,b} quinoid-type bisboron complexes **3** and **4** did not exhibit fluorescence. According to the Kasha's rule, for most photochemical processes, only the lowest excited state (S_1 or T_1) is considered as the candidate for the initiation of an emission or reaction.¹² Thus, the emissions of **3** and **4** would occur from the S_1 state, even when the allowed $S_0 \rightarrow S_2$ absorption occurs. Furthermore, the Strickler–Berg equation indicates that the radiative rate constant (k_f) is proportional to the integral of the molar extinction coefficient curve (Scheme S2).¹³ In other words, the low ϵ value decreased the k_f value; consequently, the Φ_f value decreased. The $S_0 \rightarrow S_1$ transitions of **3** and **4** are predicted to be forbidden by the TDDFT calculation ($f = 0.00$). Therefore, the nonfluorescent property of the quinoid-type bisboron complexes is probably because of the forbidden $S_0 \rightarrow S_1$ transitions that significantly decreased the k_f values.

The cyclic voltammogram of **3** is shown in Figure 4. Bisboron complex **3** underwent two successive one-electron reduction

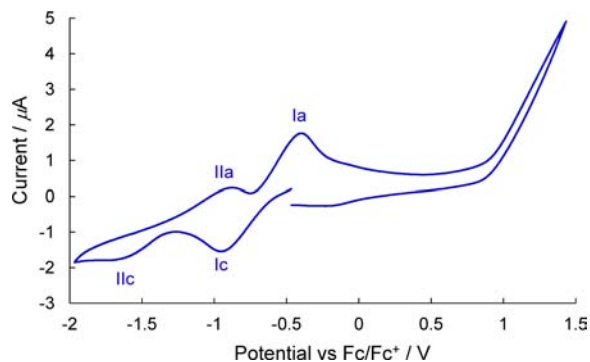


Figure 4. Cyclic voltammogram of **3** measured in THF containing tetrabutylammonium perchlorate (0.1 M) as a supporting electrolyte. AgQRE was used as a reference electrode. Platinum wire was used as the working and counter electrodes. The scan rate was 50 mV s⁻¹. Fc/Fc⁺ was used as external reference.

processes at $E_{1/2} = -0.68$ and -1.29 V (vs Fc/Fc⁺). This fact points to the formation of stable aromatic dianion of bisboron complex **6** under the applied conditions (Scheme 2). Similar result was observed for **4** (Figure S9).

Spectroelectrochemical spectrum of **3** in THF is shown in Figure 5. Bisboron complex **3** was electrochemically reduced

Scheme 2. Plausible Reaction Mechanism for the Reduction of **3**

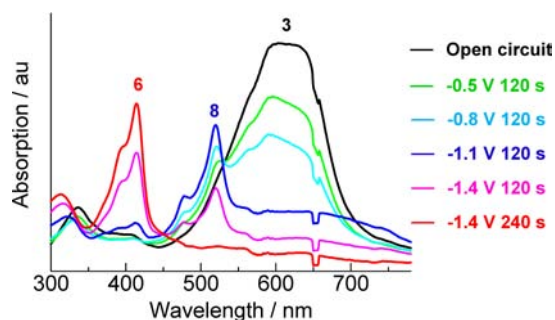
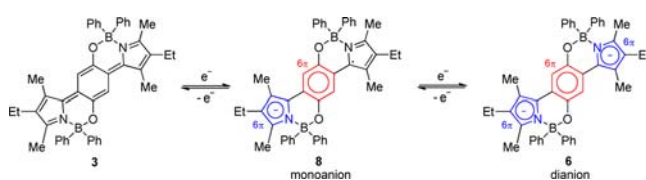


Figure 5. Electrochromic behavior of **3** in THF with tetrabutylammonium perchlorate as the supporting electrolyte at 0.0, -0.5, -0.8, -1.1, -1.4 (V vs Ag/Ag⁺ as a reference electrode). Platinum was used as the working and counter electrodes.

from 0.0 to -1.4 V (vs Ag/Ag⁺). Upon electrochemical reduction (-1.1 V vs Ag/Ag⁺), the absorption peak at ~600 nm decreased with concomitant appearance of new absorption at ~520 nm. Further reduction (-1.4 V vs Ag/Ag⁺) led to the disappearance of the peak at ~520 nm and appearance of new absorption at ~410 nm.

The TDDFT results indicated that the peaks at ~410 and 520 nm are attributed to the absorption of the dianion **6** and monoanion **8**, respectively (Table 1 and Table S2). The observed λ_{max} of **6** at 414 and 395 nm were attributable to the allowed $S_0 \rightarrow S_1$ (HOMO \rightarrow LUMO) and $S_0 \rightarrow S_3$ (HOMO \rightarrow LUMO+2) transitions, respectively. The $S_0 \rightarrow S_2$ (HOMO \rightarrow LUMO+1) transition of **6** was a forbidden transition due to no spatial overlap between the HOMO and LUMO+1 orbitals. The fact that the $S_0 \rightarrow S_1$ transition of dianion **6** is allowed predicts that **6** may show fluorescence. The observed λ_{max} of **8** at 512 nm was due to the $S_0 \rightarrow S_7$ transition (Table S2 and Figure S10). The TDDFT calculations also predicted that monoanion **8** would show absorption at ~870 nm which is attributed to the allowed $S_0 \rightarrow S_2$ transition.¹⁴

In conclusion, we synthesized novel quinoid-type bisboron complexes by two-step reactions from 1,4-benzoquinone and the corresponding pyrrole derivatives. Bisboron complexes **3** and **4** showed red-shifted λ_{max} (612–644 nm) and higher ϵ (47000–52200) values than those of ligands **1** and **2** (λ_{max} : 542–563 nm, ϵ : 22000–27300) in toluene. The TDDFT calculations revealed that these absorptions can be attributed to the $S_0 \rightarrow S_2$ transitions, which are mainly composed of HOMO–1 to LUMO transitions. The TDDFT calculations also indicated that the $S_0 \rightarrow S_1$ transitions of **3** and **4** can be mostly attributed to their HOMO–LUMO transitions; the transitions are parity forbidden, i.e., ungerade–ungerade transitions. The forbidden $S_0 \rightarrow S_1$ transition of **3** was observed at ~800 nm. Bisboron complex **3** did not exhibit any fluorescence. The nonfluorescent property of **3** is probably because of the forbidden $S_0 \rightarrow S_1$ transition. The cyclic voltammograms indicated that bisboron complex **3** is reduced to the corresponding aromatic dianion **6**. The dianion **6**

and monoanion **8** of **3** showed λ_{max} at ~ 410 and 520 nm, respectively. Although TDDFT results indicate that **8** has λ_{max} at ~ 870 nm, the NIR absorption was not observed due to the limitation of our instruments. We believe that the modification of the pyrrole ring of the bisbron complex will open doors to the development of NIR absorbing dyes having a more red-shifted absorption and NIR fluorescence dyes.

■ ASSOCIATED CONTENT

■ Supporting Information

Synthetic procedures, UV–vis absorption data, TG–DTA data, cyclic voltammograms, DFT calculation details, and X-ray crystal data. The Supporting Information is available free of charge on the ACS Publications website at DOI: 10.1021/acs.orglett.5b01547.

■ AUTHOR INFORMATION

■ Corresponding Authors

*E-mail: kubota@gifu-u.ac.jp.

*E-mail: matsui@gifu-u.ac.jp.

■ Notes

The authors declare no competing financial interest.

■ ACKNOWLEDGMENTS

This work was partially supported by JSPS KAKENHI (25870293, Grant-in-Aid for Young Scientists (B)).

■ REFERENCES

- (1) (a) Fabian, J.; Nakazumi, H.; Matsuoka, M. *Chem. Rev.* **1992**, *92*, 1197. (b) Qian, G.; Wang, Z. *Y. Chem.—Asian J.* **2010**, *5*, 1006. (c) Fabian, J. *Dyes Pigm.* **2010**, *84*, 36.
- (2) (a) Yuan, Z.; Lee, S.-L.; Chen, L.; Li, C.; Mali, K. S.; De Feyter, S.; Müllen, K. *Chem.—Eur. J.* **2013**, *19*, 11842. (b) Panigrahi, M.; Dash, S.; Patel, S.; Mishra, B. K. *Tetrahedron* **2012**, *68*, 781. (c) Furuyama, T.; Satoh, K.; Kushiya, T.; Kobayashi, N. *J. Am. Chem. Soc.* **2014**, *136*, 765. (d) Shchepinov, M. S.; Korshun, V. A. *Chem. Soc. Rev.* **2003**, *32*, 170.
- (3) (a) Frath, D.; Massue, J.; Ulrich, G.; Ziessel, R. *Angew. Chem., Int. Ed.* **2014**, *53*, 2290. (b) Li, D.; Zhang, H.; Wang, Y. *Chem. Soc. Rev.* **2013**, *42*, 8416. (c) Loudet, A.; Burgess, K. *Chem. Rev.* **2007**, *107*, 4891. (d) Chibani, S.; Le Guennic, B.; Charaf-Eddin, A.; Laurent, A. D.; Jacquemin, D. *Chem. Sci.* **2013**, *4*, 1950. (e) Wakamiya, A.; Mori, K.; Yamaguchi, S. *Angew. Chem., Int. Ed.* **2007**, *46*, 4273. (f) Yoshii, R.; Nagai, A.; Tanaka, K.; Chujo, Y. *Chem.—Eur. J.* **2013**, *19*, 4506. (g) Fischer, G. M.; Ehlers, A. P.; Zumbusch, A.; Daltrozzi, E. *Angew. Chem., Int. Ed.* **2007**, *46*, 3750. (h) Ono, K.; Yoshikawa, K.; Tsuji, Y.; Yamaguchi, H.; Uozumi, R.; Tomura, M.; Taga, K.; Saito, K. *Tetrahedron* **2007**, *63*, 9354.
- (4) (a) Zhang, Z.; Bi, H.; Zhang, Y.; Yao, D.; Gao, H.; Fan, Y.; Zhang, H.; Wang, Y.; Wang, Y.; Chen, Z.; Ma, D. *Inorg. Chem.* **2009**, *48*, 7230. (b) Li, D.; Wang, D.; Huang, S.; Qu, S.; Liu, X.; Zhu, Q.; Zhang, H.; Wang, Y. *J. Mater. Chem.* **2011**, *21*, 15298. (c) Li, D.; Yuan, Y.; Bi, H.; Yao, D.; Zhao, X.; Tian, W.; Wang, Y.; Zhang, H. *Inorg. Chem.* **2011**, *50*, 4825. (d) Li, D.; Zhang, H.; Wang, C.; Huang, S.; Guo, J.; Wang, Y. *J. Mater. Chem.* **2012**, *22*, 4319.
- (5) (a) Frath, D.; Azizi, S.; Ulrich, G.; Retailleau, P.; Ziessel, R. *Org. Lett.* **2011**, *13*, 3414. (b) Frath, D.; Azizi, S.; Ulrich, G.; Ziessel, R. *Org. Lett.* **2012**, *14*, 4774. (c) Massue, J.; Frath, D.; Ulrich, G.; Retailleau, P.; Ziessel, R. *Org. Lett.* **2012**, *14*, 230. (d) Massue, J.; Retailleau, P.; Ulrich, G.; Ziessel, R. *New J. Chem.* **2013**, *37*, 1224. (e) Massue, J.; Ulrich, G.; Ziessel, R. *Eur. J. Org. Chem.* **2013**, 5701. (f) Benelhadj, K.; Massue, J.; Retailleau, P.; Ulrich, G.; Ziessel, R. *Org. Lett.* **2013**, *15*, 2918. (g) Massue, J.; Frath, D.; Retailleau, P.; Ulrich, G.; Ziessel, R. *Chem.—Eur. J.* **2013**, *19*, 5375.
- (6) (a) Hou, Q.; Zhao, L.; Zhang, H.; Wang, Y.; Jiang, S. *J. Lumin.* **2007**, *126*, 447. (b) Kim, S.-H.; Gwon, S.-Y.; Burkinshaw, S. M.; Son, Y.-A. *Dyes Pigm.* **2010**, *87*, 268. (c) Son, H.-J.; Han, W.-S.; Wee, K.-R.; Chun, J.-Y.; Choi, K.-B.; Han, S. J.; Kwon, S.-N.; Ko, J.; Lee, C.; Kang, S. O. *Eur. J. Inorg. Chem.* **2009**, 1503. (d) Kwak, M. J.; Kim, Y. *Bull. Korean Chem. Soc.* **2009**, *30*, 2865. (e) Ma, R.-Z.; Yao, Q.-C.; Yang, X.; Xia, M. *J. Fluorine Chem.* **2012**, *137*, 93. (f) Santra, M.; Moon, H.; Park, M.-H.; Lee, T.-W.; Kim, Y. K.; Ahn, K. H. *Chem.—Eur. J.* **2012**, *18*, 9886. (g) Li, X.; Son, Y.-A. *Dyes Pigm.* **2014**, *107*, 182.
- (7) (a) Kubota, Y.; Tsuzuki, T.; Funabiki, K.; Ebihara, M.; Matsui, M. *Org. Lett.* **2010**, *12*, 4010. (b) Kubota, Y.; Uehara, J.; Funabiki, K.; Ebihara, M.; Matsui, M. *Tetrahedron Lett.* **2010**, *51*, 6195. (c) Kubota, Y.; Hara, H.; Tanaka, S.; Funabiki, K.; Matsui, M. *Org. Lett.* **2011**, *13*, 6544. (d) Kubota, Y.; Tanaka, S.; Funabiki, K.; Matsui, M. *Org. Lett.* **2012**, *14*, 4682. (e) Kubota, Y.; Ozaki, Y.; Funabiki, K.; Matsui, M. *J. Org. Chem.* **2013**, *78*, 7058. (f) Kubota, Y.; Sakuma, Y.; Funabiki, K.; Matsui, M. *J. Phys. Chem. A* **2014**, *118*, 8717. (g) Kubota, Y.; Kasatani, K.; Takai, H.; Funabiki, K.; Matsui, M. *Dalton Trans.* **2015**, *44*, 3326.
- (8) (a) Bullock, E. *Can. J. Chem.* **1958**, *36*, 1744. (b) Bonnett, R.; Motevalli, M.; Siu, J. *Tetrahedron* **2004**, *60*, 8913. (c) Fischer, H.; Treibs, A.; Zaucker, E. *Chem. Ber.* **1959**, *92*, 2026.
- (9) Kudo, K.; Momotake, A.; Kanna, Y.; Nishimura, Y.; Arai, T. *Chem. Commun.* **2011**, 3867.
- (10) Frisch, M. J.; Trucks, G. W.; Schlegel, H. B.; Scuseria, G. E.; Robb, M. A.; Cheeseman, J. R.; Montgomery, J. A., Jr.; Vreven, T.; Kudin, K. N.; Burant, J. C.; Millam, J. M.; Iyengar, S. S.; Tomasi, J.; Barone, V.; Mennucci, B.; Cossi, M.; Scalmani, G.; Rega, N.; Petersson, G. A.; Nakatsuji, H.; Hada, M.; Ehara, M.; Toyota, K.; Fukuda, R.; Hasegawa, J.; Ishida, M.; Nakajima, T.; Honda, Y.; Kitao, O.; Nakai, H.; Klene, M.; Li, X.; Knox, J. E.; Hratchian, H. P.; Cross, J. B.; Adamo, C.; Jaramillo, J.; Gomperts, R.; Stratmann, R. E.; Yazyev, O.; Austin, A. J.; Cammi, R.; Pomelli, C.; Ochterski, J. W.; Ayala, P. Y.; Morokuma, K.; Voth, G. A.; Salvador, P.; Dannenberg, J. J.; Zakrzewski, V. G.; Dapprich, S.; Daniels, A. D.; Strain, M. C.; Farkas, O.; Malick, D. K.; Rabuck, A. D.; Raghavachari, K.; Foresman, J. B.; Ortiz, J. V.; Cui, Q.; Baboul, A. G.; Clifford, S.; Cioslowski, J.; Stefanov, B. B.; Liu, G.; Liashenko, A.; Piskorz, P.; Komaromi, I.; Martin, R. L.; Fox, D. J.; Keith, T.; Al-Laham, M. A.; Peng, C. Y.; Nanayakkara, A.; Challacombe, M.; Gill, P. M. W.; Johnson, B.; Chen, W.; Wong, M. W.; Gonzalez, C.; Pople, J. A. *Gaussian 09, Revision A. 02*; Gaussian, Inc.: Wallingford, CT, 2009.
- (11) (a) Laporte, O.; Meggers, W. F. *J. Opt. Soc. Am.* **1925**, *11*, 459. (b) Tsuboi, Y.; Shimizu, R.; Shoji, T.; Kitamura, N. *J. Am. Chem. Soc.* **2009**, *131*, 12623.
- (12) (a) Kasha, M. *Disc. Faraday Soc.* **1950**, *9*, 14. (b) Turro, N. J. *Modern Molecular Photochemistry*; University Science Books: Sausalito, 1991.
- (13) (a) Strickler, S. J.; Berg, R. A. *J. Chem. Phys.* **1962**, *37*, 814. (b) Fukazawa, A.; Hara, M.; Okamoto, T.; Son, E.-C.; Xu, C.; Tamao, K.; Yamaguchi, S. *Org. Lett.* **2008**, *10*, 913.
- (14) Unfortunately, the NIR absorption could not be measured due to the limitation of our instruments.